

# Electrocorticographic–Histopathologic Correlations Implying Epileptogenicity of Dysembryoplastic Neuroepithelial Tumor

Kota KAGAWA,<sup>1</sup> Koji IIDA,<sup>1</sup> Akiyoshi KAKITA,<sup>2</sup> Masaya KATAGIRI,<sup>1</sup>  
Takeshi NISHIMOTO,<sup>1</sup> Akira HASHIZUME,<sup>1</sup> Yoshihiro KIURA,<sup>1</sup> Ryosuke HANAYA,<sup>3</sup>  
Kazuhiko SUGIYAMA,<sup>1</sup> Koji ARIHIRO,<sup>4</sup> Kazunori ARITA,<sup>3</sup> and Kaoru KURISU<sup>1</sup>

<sup>1</sup>Department of Neurosurgery, Graduate School of Biomedical and Health Sciences,  
Hiroshima University, Hiroshima, Hiroshima;

<sup>2</sup>Department of Pathology, Brain Research Institute,  
University of Niigata, Niigata, Niigata;

<sup>3</sup>Department of Neurosurgery, Graduate School of Medical and Dental Sciences,  
Kagoshima University, Sakuragaoka, Kagoshima;

<sup>4</sup>Department of Pathology, Graduate School of Biomedical Sciences,  
Hiroshima University, Hiroshima, Hiroshima

## Abstract

Based on intracranial-video electroencephalography (EEG), histopathological features, and postoperative seizure outcome, we elucidated the epileptogenicity in patients with dysembryoplastic neuroepithelial tumor (DNT). Five patients (P1–P5) pathologically diagnosed with DNT underwent intracranial-video EEG to identify the ictal onset zone and irritative zone. We evaluated the correlations of ictal onset zone and irritative zone with the magnetic resonance imaging-visible lesion (MRI-lesion) and their histopathological features. Intracranial-video EEG located the ictal onset zone adjacent to the MRI-lesion margin in four patients with complex/simple forms of DNT subcategory, and on the MRI-lesion in P3 with a nonspecific DNT form. The irritative zone extended to surrounding regions of the ictal onset zone in all patients. Histopathologically, MRI-lesions were characterized by specific glioneuronal elements, whereas the ictal onset zone and irritative zone were represented with dysplastic cortex accompanying oligodendroglia-like cells in four (P1, P2, P4, and P5) of five patients. Cortical dysplasia was identified with typical histopathologic features in the irritative zone remote from the MRI-lesion in P5. P3, with a nonspecific form, indicated prominent component of dysplastic cortex with oligodendroglia-like cells scattered in the MRI-lesion. Lesionectomy of MRI-lesion with additional cortical resections (including the ictal onset zone and irritative zone) yielded postoperative seizure freedom (Engel Class I) in P3, P4, and P5, while P1 and P2 (with only lesionectomy) experienced postoperative residual seizure (Class II and III in each patient). Our results suggest the intrinsic epileptogenicity of DNT. The topographical correlation indicated that the dysplastic cortex accompanying oligodendroglia-like cells was more epileptogenic than the specific glioneuronal elements itself. Meticulous intracranial-video EEG analysis delineating the MRI nonvisible ictal onset zone and the irritative zone may yield better seizure outcome.

Key words: dysembryoplastic neuroepithelial tumor (DNT), epileptogenicity, epilepsy surgery, intracranial electroencephalography (EEG), histopathology

## Introduction

The highly epileptogenic dysembryoplastic neuroepithelial tumor (DNT) arises from the cortical area of most frequently the temporal lobe at a young age.<sup>5,6)</sup>

DNT consists of a mixture of glial and neuronal elements pathologically characterized by a specific glioneuronal element with/without glial nodules and a multinodular architecture.<sup>6)</sup> Oligodendroglia-like cells, a prominent constituent cell type of specific glioneuronal element, are arranged along the capillaries in compact or loose alveolar areas.

Mature neurons are unitarily dispersed in a mucoid matrix.<sup>5,6,12,15</sup> Dumas-Duport et al. have originally described two histopathologic forms of DNT: simple and complex.<sup>5,6</sup> The former exhibits only specific glioneuronal element,<sup>5,6</sup> while the latter contains specific glioneuronal element as a main feature and multinodular architecture of glial nodules resembling astrocytomas, oligodendrogliomas, or oligoastrocytomas.<sup>5,6</sup> The foci of cortical dysplasia are commonly located in the adjacent brain sites of both forms.<sup>6</sup> Previous studies have reported that the epileptogenicity of DNT may be attributable to coexisting cortical dysplasia<sup>14,17,24,26</sup>; however, the precise localization of epileptogenicity remains unclear to date.<sup>17</sup> The option of adopting a surgical strategy for DNT-related intractable epilepsy is still controversial: some advocate that lesionectomy of a DNT lesion is enough to remit seizures,<sup>1,6,10,16</sup> while others prefer an extended resection associated with the epileptogenic cortex for better seizure outcome.<sup>4,14,17,23,24,26,27</sup>

Previous data on intraoperative electrocorticography (ECoG) showing active interictal spiking in the cortical areas adjacent to the DNT lesion appear to support the extended resection strategy.<sup>9,14,17,26,27</sup> Few studies have evaluated the correlation between DNT and epileptogenic foci using extraoperative ECoG.<sup>14,23</sup> The epileptogenic foci corresponding to either the ictal onset zone or irritative zone were not located within the DNT lesions, rather they were detected more frequently in the cortex nearby.

Hitherto, studies on correlations between the interictal/ictal ECoG findings and cortical topography of histopathologic elements associated with DNT have not been attempted.<sup>5–7,12</sup> In this retrospective study, we correlated the histopathologic findings of DNT, including the magnetic resonance imaging-visible lesion (MRI-lesion) and the surrounding tissues of the ictal onset zone and irritative zone acquired in DNT patients, who had undergone epilepsy surgery via extraoperative intracranial-video electroencephalography (EEG) monitoring.

## Patients and Methods

### I. Patients

We enrolled five male patients (P1–P5) who had undergone epilepsy surgery secondary to DNT between April 2003 and March 2009. Table 1 provides a summary of the clinical profiles of patients (age range: 11–41 years; mean: 23 years). Their seizure durations ranged from 15 months to 19 years (mean: 14.3 years). Four patients (P1, P2, P3, and P5; with P3 suffering from auditory seizure) had clinical

histories and ictal symptoms of partial seizures with secondary generalization, while P4 suffered from only partial seizures. Although other patients experienced one or more seizures per month, P3 had daily seizures. All patients themselves or their next-of-kin gave informed consent.

In presurgical evaluation, all patients underwent MRI, prolonged scalp-video EEG (SVEEG) monitoring, magnetoencephalography (MEG), neuropsychological examination, and the Wada test for determining the language-dominant hemisphere. Preoperative MRI was performed using a 1.5T MRI (Signa or Signa Horizon, GE Medical Systems, Waukesha, Wisconsin, USA). The epilepsy protocol included the following sequences: axial T<sub>1</sub>-weighted; axial and coronal T<sub>2</sub>-weighted; as well as axial and coronal fluid-attenuated inversion-recovery (FLAIR). Gadolinium-based contrast was injected intravenously in all patients.

We performed prolonged SVEEG (BMSI 4000 and 6000, Nicolet Biomedical Inc., Madison, Wisconsin, USA) with the International 10–20 scalp-electrode placement system using a single reference electrode and sphenoidal electrodes whenever necessary. We studied MEG using the Neuromag System (a whole-head 306-channel type, Elekta-Neuromag O.Y., Helsinki, Finland) including 204-channel planar gradiometers. MEG data were analyzed with an equivalent current dipole (ECD) model to locate the epileptic spike sources.

### II. Extraoperative intracranial-video EEG

We performed extraoperative intracranial-video EEG in all patients for 5–9 days to localize the epileptic zone and map the functionally eloquent areas. After craniotomy, a subdural grid electrode was placed accordingly. The area covered was decided based on MRI findings, interictal/ictal SVEEG results, sites of MEG spike sources, and clinical symptoms. Contiguous monitoring of the neocortical areas or mesiobasal temporal regions was done through the placement of adjacent electrodes without leaving any intervening unsampled cortical area. We defined the ictal onset zone as a site where low-amplitude fast waves or rhythmic spikes were initiated preceding clinical behavior,<sup>25</sup> and the irritative zone is a site where synchronized spike discharges at three or more intracranial electrodes were interictally recorded.<sup>13</sup> The epileptic zones on intracranial-video EEG were defined as the ictal onset zone and irritative zone. We used the following types of intracranial electrodes (Unique Medical, Tokyo) for recording: grid electrode, strip electrode, depth electrode, and mesial temporal type electrode. The mesial temporal type electrode for monitoring the mesial and basal temporal regions recorded the two

**Table 1 Clinical profile of patients and correlation of MR imaging to prolonged SVEEG and MEG findings**

Patient No.	Age/ Sex	Duration of epilepsy	Clinical profile		MRI			Prolonged SVEEG		MEG
			Seizure semiology	Seizure frequency	Location	Findings	Interictal zone	Ictal onset zone	Location of ECD cluster	
1	11/M	9 yr	CPS with R head version and R arm dystonic posturing, SG	2-3/mo	L lat T	Hyperintensity on T2 WI; well-defined border; multinodular	Generalized	Generalized	Generalized	Posterior to MRI-L
2	11/M	8 yr	CPS with L tonic arm extension, SG	1-2/mo	R lat T	Hyperintensity on T2 WI; well-defined border; multinodular	R post T-O	R post T-O	R post T-O	Posterior to MRI-L
3	14/M	15 mo	SPS (auditory hallucination), SG	4-5/day	R lat T	Hyperintensity on T2 WI; slightly indistinct border; single nodule	R C-mid T	R C-mid T	R C-mid T	No spikes
4	41/M	29 yr	CPS with orolimentary automatism and vocalization	1-2/week	L mes T	Hyperintensity on T2 WI; well-defined border; single nodule	Independent L and R ant T-sub T	Independent L and R ant T-sub T	Independent L and R ant T-sub T	No spikes
5	36/M	24 yr	CPS with R arm dystonic posturing, L hand automatism, and orolimentary automatism, SG	1-2/mo	L mes T, insula; basal F	Hyperintensity on T2 WI (heterogeneous); lightly indistinct border; multinodular; multicystic	L ant T-sub T	L ant T-sub T	L ant T-sub T	L ant T

ant: anterior, CPS: complex partial seizure, ECD: equivalent current dipole, F: frontal, L: left, lat: lateral, MEG: magnetoencephalography, mes: mesial, mo: month(s), MRI: magnetic resonance imaging, MRI-L: MRI-visible lesion, O: occipital, post: posterior, R: right, SG: secondary generalized seizure, SPS: simple partial seizure, SVEEG: scalp-video electroencephalography, T: temporal, WI: weighted image, yr: year(s).

four-contact arrays with an orthogonal axis: distal part for the mesial temporal region and proximal for the strip electrodes. The depth electrode was directly inserted into the hippocampus or MRI-lesion, when and where necessary. The extents of ictal onset zone and irritative zone were evaluated by the number of electrodes involved.

### III. Localization of intracranial electrodes: positioning by using digital camera-derived intraoperative images and MRI-based three-dimensional reconstruction

We performed intracranial electrode positioning by using digital camera-derived intraoperative images according to the methods described previously.<sup>22)</sup> A digital camera image of the brain surface was first obtained (Fig. 1A) before procuring another image after the intracranial electrodes were placed (Fig. 1B). Based on the results of intracranial-video EEG monitoring, we mapped out an epileptic

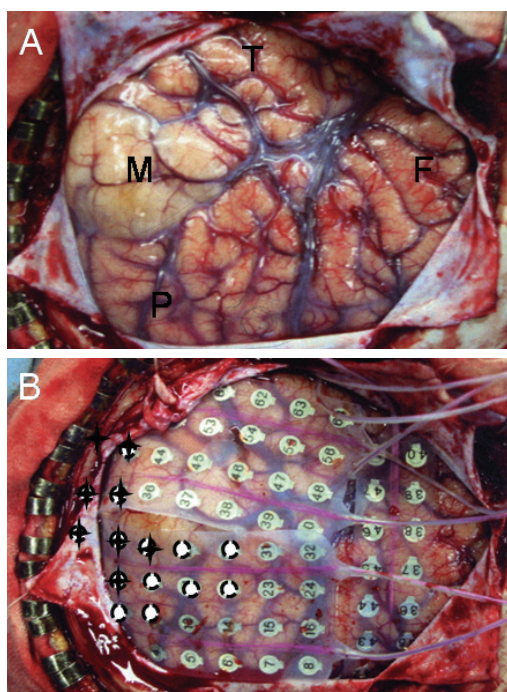


**Fig. 1** Localization of the intracranial electrode positions by using digital camera-derived intraoperative images and magnetic resonance imaging (MRI)-based three-dimensional reconstruction in P1. A: Brain surface at the first craniotomy shows a white-tinged cortical lesion corresponding to the MRI-visible lesion (M: MRI-lesion, T: temporal lobe, F: frontal lobe, P: parietal lobe). B: An image of the brain surface after intracranial electrode positioning. The electrodes were marked as crosses for the ictal onset zones and white-filled dotted circles for the irritative zones.

zone (ictal onset zone and irritative zone) and the functional site on the digital camera-acquired image. All five patients had MRI studies after intracranial-video EEG monitoring to elucidate the positional relationships between the MRI-lesion and intracranial electrodes in a two-dimensional (2D) fashion. Furthermore, the three-dimensional (3D) surface reconstruction of patient's individual brain was created to provide visual correlation between each intracranial electrode position and the corresponding cortical area and the MRI-lesion. To obtain 3D brain volume data, we used spoiled gradient recalled acquisitions in the steady state. From such MRI data, we manually segmented the brain voxels (1 mm<sup>3</sup> voxels) and calculated the volume derived from segmented voxels rendering the brain image. We manually plotted locations of the electrode contacts (represented by small circles) and the MRI-lesions (represented by dotted lines if the lesion was deep-seated) on the reconstructed brain surface by comparing the digital camera-acquired images and 2D MR images. This reconstruction fused with the plotted electrodes and the MRI-lesion allowed accurate identification of the MRI-lesion, ictal onset zone, and irritative zone sites (Fig. 2).

### IV. Surgical procedures and histopathologic studies

Our surgical strategy for the DNT-related epilepsy adopted lesionectomy with additional and possibly complete cortical resection of the epileptic zone. In this study, the term “lesionectomy” implied resection of the MRI-lesion, and the term “cortical resection” meant resection of the epileptic zone including the ictal onset zone and irritative zone (as defined before). The final extent of cortical resection was based on the results of intracranial-video EEG and the location of functionally eloquent areas.

After the second craniotomy, nondisplacement of the intracranial electrode positions on the brain surface was confirmed by comparing with the digital camera-acquired image (taken in the first craniotomy and MRI-based 3D reconstruction images fused with the electrodes described above). On removal of the electrodes, the ictal onset zone and irritative zone were demarcated with a white suture encircling the brain surface sites where electrodes had previously been placed. We tried *en bloc* resection of the MRI-lesion (note that the resected tissue bloc varied in size and number with the surgical procedures adopted for each patient). The tissues were accordingly labeled as MRI-lesion, ictal onset zone, and irritative zone. Two patients (P4 and P5) with mesial temporal

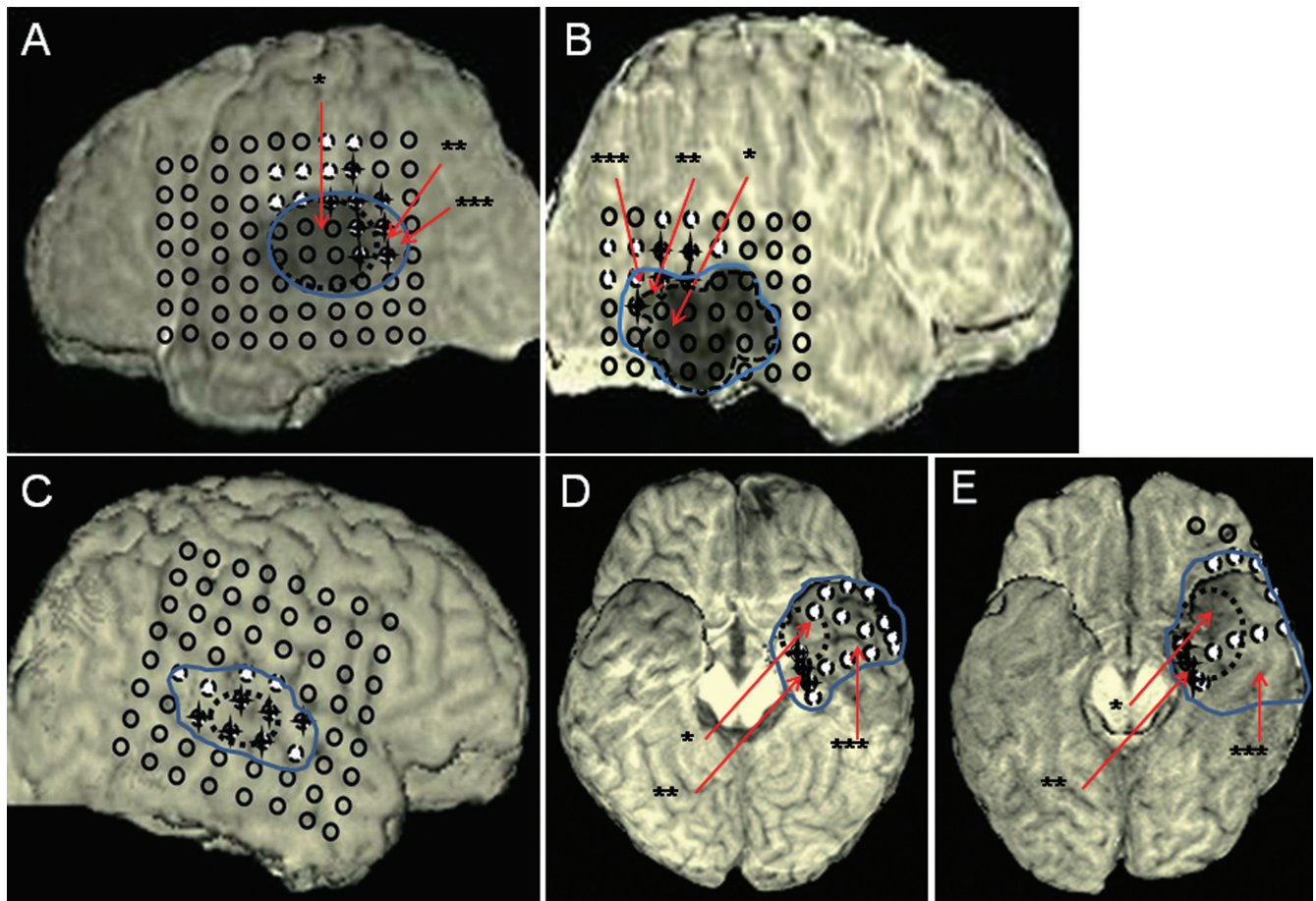


**Fig. 2** Reconstructed brain surface shows magnetic resonance imaging-visible lesions (MRI-lesions) (*dotted circles*), superimposed ictal onset zone and irritative zone-related intracranial electrodes (ictal onset zones marked with *crosses*; irritative zones marked with *white-filled dotted circles*), and resected area (*blue circles*). **A (P1):** Ictal onset zones were present at the spuramarginal gyrus and angular gyrus adjacent to the MRI-lesion, while irritative zones were distributed more extensively (surrounding the MRI-lesions). **B (P2):** Ictal onset zones were present at the middle temporal gyrus and angular gyrus adjacent to the MRI-lesion, while irritative zones were distributed more extensively (surrounding the MRI-lesions). **C (P3):** The ictal onset zones and irritative zones were present within the surface of the MRI-lesion and contiguously extended to areas adjacent to the gyri. **D (P4):** Ictal onset zones were present at the parahippocampal gyrus adjacent to the MRI-lesion, while irritative zones were distributed more extensively (including basal and lateral temporal regions). **E (P5):** Ictal onset zones were present at the parahippocampal gyrus adjacent to the MRI-lesion, while irritative zones were distributed more extensively (including basal and lateral temporal regions and basal frontal regions). Pathological features of different resected area in the same patient corresponded well to specific glioneuronal elements with (P5) or without (P1, P2, and P4) astrocyte proliferation and calcification (*asterisk*), dysplastic cortex accompanying oligodendroglia-like cells (*double asterisks*), and normal looking cortex (*triple asterisks*). Such pathological findings of a gradual transitional form are demonstrated in Fig. 4.

DNT underwent resection of the mesial structures due to the hippocampal involvement of DNT. Tissues were then fixed with phosphate-buffered 20% formalin and embedded in paraffin wax before 5- $\mu$ m-thick sections were serially cut and stained with hematoxylin and eosin or Klüver-Barrera stain.

## V. Seizure outcome

The postoperative seizure outcome was graded according to the Engel's classifications: free of disabling seizures (Class I); rare disabling seizures (Class II); worthwhile improvement (Class III); or no worthwhile improvement (Class IV).<sup>8)</sup>

## Results

### I. MRI, prolonged SVEEG, and MEG findings

All five patients underwent MRI examinations (Table 1). The MRI-lesions were present in the lateral temporal region of three (P1, P2, and P3) and in the mesial temporal region of two patients (P4 and P5). The lesions were characterized with T<sub>2</sub>-weighted and FLAIR hyperintensity with well-defined borders to the surrounding cortex and multinodular in three patients (P1, P2, and P4) (Fig. 3A), a slightly indistinct border to the surrounding cortex (Fig. 3C) was observed in one patient (P3), and a heterogeneous multicystic pattern (Fig. 3D) was noted in another patient (P5).

Based on the results (Table 1), prolonged SVEEG localized interictal epileptiform discharges (corre-

sponding anatomically to the location of MRI-lesion) in P2, P3, and P5. One patient (P4) had independent epileptiform discharges from the bilateral anterior temporal and subtemporal regions. Generalized epileptiform discharges occurred in one patient (P1). Seizure onsets occurred independently in the bilateral anterior temporal and subtemporal regions in one patient (P4), although the seizure semiology was consistent in all seizures. P1 had nonlocalized ictal onset zones with diffusely rhythmic bilateral synchronous discharges.

In distributions of the ECD cluster area on MEG in relation to the MRI-lesion (Table 2), three patients (P1, P2, and P5) manifested single ECD clusters. Two patients (P1 and P2) displayed the ECD clusters contiguously extended to the MRI-lesions (Fig. 3B). P5 with MRI-lesion in the mesial temporal region exhibited an ECD cluster with horizontal moment in the anterior temporal region. No MEG spikes were recorded in the other two patients (P3 and P4).

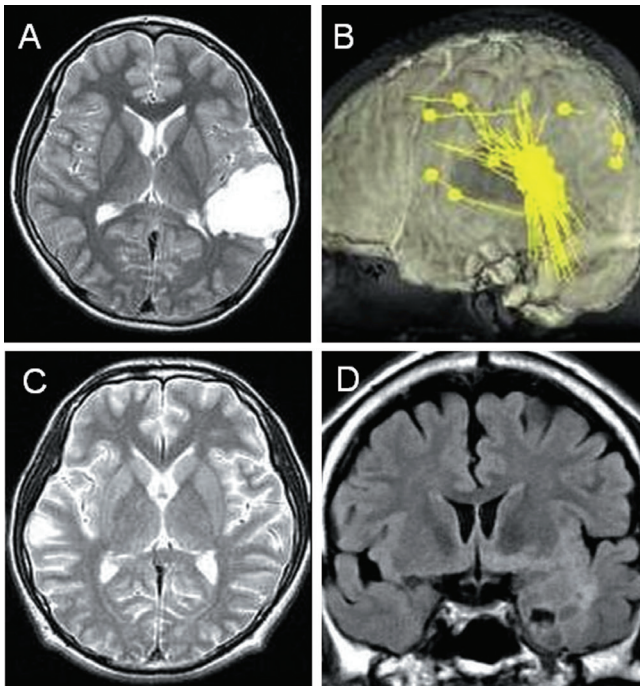


**Fig. 3** A: An axial T<sub>2</sub>-weighted image portrays a multinodular lesion with well-defined hyperintensity in the left superior and middle temporal gyri in P1 (see Fig. 1). B: Equivalent current dipoles (ECDs) of interictal magnetoencephalography spikes superimposed on the reconstructed brain surface in P1 (see Fig. 1). Note that the ECDs were clustered posterior to the magnetic resonance imaging (MRI)-visible lesion. C: MRI in P3 reveals T<sub>2</sub>-weighted hyperintensity lesions with a slightly indistinct border in the right superior to middle temporal gyri. D: Coronal fluid-attenuated inversion-recovery image of P5 shows a heterogeneous hyperintensity lesion with a multicystic component and slightly indistinct border involving the left anterior to mesial temporal, insula, and basal frontal regions.

### II. Epileptic zones on intracranial-video EEG in correlation to the MRI-lesions

All patients underwent intracranial-video EEG before lesionectomy with/without additional cortical resection. Table 2 shows the correlations between the MRI-lesion with intracranial-video EEG findings. Subdural grid electrodes were used in all patients. Supplemental electrodes were used in two patients for intracranial-video EEG in the mesial temporal structures (P4 and P5), and in the basal frontal region and insular cortex (P5). Intracranial-video EEG localized the ictal onset zone and irritative zones in all patients. Four patients (P1, P2, P4, and P5) had ictal onset zones where the distributions were limited to the adjacent gyrus or two gyri to the MRI-lesion (Fig. 2A, B, D, E). P3, whose pathologic diagnosis of the resected specimen was that of a nonspecific form of DNT, indicated ictal onset zone distributions different from those of the other four patients. The ictal onset zone in P3 was located within the MRI-lesion and extended contiguously to the adjacent gyri (Fig. 2C). The number of ictal onset zone-related electrodes ranged between 3 and 8 (Table 2). Irritative zones in all patients overlapped with the ictal onset zones, albeit they extended more contiguously beyond the ictal onset zone and MRI-lesions (Fig. 2A–E). The number of irritative zone-related electrodes ranged between 11 and 31.

### III. Histopathologic findings and their correlations to intracranial-video EEG and MRI

Histopathological examination of surgical specimens revealed that the lesions in four of five patients showed characteristics typical of DNT (Table 2); the lesions

Table 2 Electrocticographic-histopathologic correlations and surgical outcomes

Patient No.	Diagnosis	MRI-L			IOZ		IZ		Surgery	
		Location	Pathological main component	Location	Number of electrode involved (type of electrode)	Pathological features	Location	Number of electrode involved (type of electrode)	Pathological features	Procedure
1	DNT (simple form)	L STG and MTG	SGNE	Sup-marginal G and angular G	8 (Ge)	Sup-marginal G and angular G	15 (Ge)	NA	Total lesionectomy with partial removal of IOZ and IZ	Class III/104 mo
2	DNT (simple form)	R MTG and ITG	SGNE	MTG and angular G	5 (Ge)	MTG and angular G	12 (Ge)	NA	Total lesionectomy with partial removal of IOZ and IZ, and MST	Class II/99 mo
3	DNT (nonspecific form)	R STG and MTG	CD intermixed by OLC	STG and MTG	6 (Ge)	CD intermixed by OLC	11 (Ge)	CD intermixed by OLC	Total lesionectomy with complete removal of IOZ and IZ	Class I/87 mo
4	DNT (simple form)	L HPC	SGNE	PHG	3 (SMe)	PHG, FG, ITG, MTG, and STG	14 (Ge), 12 (Se), 4 (SMe)	Gradual transition from IOZ to well-preserved cortex	Total lesionectomy with complete removal of IOZ and IZ	Class I/53 mo
5	DNT (complex form)	L HPC, PHG, AMY, insula, and basal F	SGNE, astrocyte proliferation and calcification	PHG	3 (SMe)	PHG, FG, ITG, MTG, and STG	16 (GE), 8 (Se), 4 (SMe), 3 (De)	Gradual transition from IOZ to well-preserved cortex, and foci of CD remote from MRI-L	Partial lesionectomy with complete removal of IOZ and IZ	Class I/34 mo

\*Engel's classification. AMY: amygdala, angular G: gyrus, CD: cortical dysplasia, De: depth electrode, F-base: frontal base, FG: fusiform gyrus, Ge: grid electrode, HPC: hippocampus, IOZ: ictal onset zone, ITG: inferior temporal gyrus, IZ: irritative zone, L: left, mo: months, MRI-L: MRI-visible lesion, MST: multiple subpial transection, MTG: middle temporal gyrus, NA: not applicable, OLCs: oligodendroglia-like cells, PHG: parahippocampal gyrus, R: right, Se: strip electrode, SGNE: specific glioneuronal element, SMe: strip electrode for mesial temporal region, STG: superior temporal gyrus, Sup-marginal G: supramarginal gyrus.

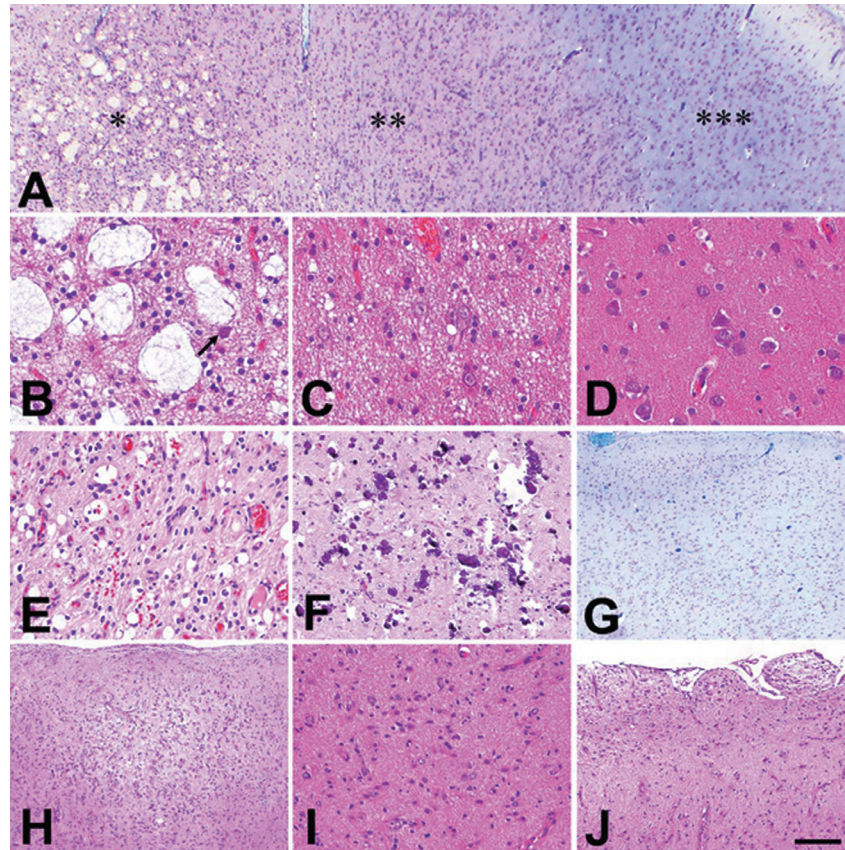


**Fig. 4** Photomicrographs of the simple form (A–D) in P1, complex form (E–G) in P5, and nonspecific form (H–J) in P3 with a dysembryoplastic neuroepithelial tumor are indicated. A low-power view demonstrates a gradual transition from the specific glioneuronal elements (*asterisk*) to normal-looking cortex (*triple asterisks*) via the dysplastic cortex (*double asterisks*). A higher-power view of the specific glioneuronal element portrays oligodendroglia-like cells with a floating neuron (*arrow*) (B), the dysplastic cortex with several oligodendroglia-like cells and vacuolated neuropils (C), and relatively well-preserved cortical areas (D). The areas of the specific glioneuronal element and dysplastic cortex correspond well to the magnetic resonance imaging-visible lesion (MRI-lesion) and ictal onset/irritative zones, respectively. Areas of astrocyte proliferation (E) and calcification (F) correspond well to the ictal onset/irritative zones adjacent to the MRI-lesion. A low-magnification view (G) of the lateral temporal cortex indicates architectural abnormalities. The cortex corresponds to the irritative zone, apart from the MRI-lesion. A nodular cortical lesion showing dysplasia with several oligodendroglia-like cells but lacking mucinous background is observed (H). Proliferation of astrocytic cells with hyperchromatic nucleus and processes (I) is noted. A superficial cortical layer shows astrocytic cells with increased cellularity (J). The lesions correspond well to the MRI-visible lesions and ictal onset/irritative zones. Staining with the Klüver–Barrera reagent (A, G) and hematoxylin and eosin reagent (B–F, H–J) were performed accordingly. The bar (J) represents 170  $\mu\text{m}$  (A), 40  $\mu\text{m}$  (B–D), 80  $\mu\text{m}$  (E and I), 160  $\mu\text{m}$  (F and J), 800  $\mu\text{m}$  (G), and 320  $\mu\text{m}$  (H), respectively.

in three patients (P1, P2, and P4) were categorized as the simple form,<sup>5,6</sup> where the specific glioneuronal element was observed as a predominant feature (Fig. 4A–D). Within the lesion in P5, nodular proliferation of astrocytes resembling astrocytoma (Fig. 4E) and marked calcification (Fig. 4F) were evident; that is, features compatible with those of the complex form.<sup>5,6</sup>

In correlations of MRI with intracranial-video EEG in these patients (Table 2), MRI-lesions indi-

cated specific glioneuronal elements with (P5) or without (P1, P2, P4) astrocyte proliferation and calcification. We have composited maps of four patients (P1, P2, P4, and P5) in Fig. 2 to correlate the resection area (MRI-lesion, ictal onset zone, and irritative zone) to histopathological findings. The ictal onset zones detected in the cortex adjacent to the MRI-visible specific glioneuronal element lesions were histopathologically composed of dysplastic



cortex with a variable number of oligodendroglia-like cells (Fig. 4A, C). Moreover, irritative zones covering the ictal onset zones and surrounding areas histopathologically corresponded to the dysplastic cortex and their contiguous normal-looking cortical areas (Fig. 4A, D). In P5 (with complex form DNT and specific glioneuronal element), astrocyte proliferation and calcification were also evident in the ictal onset zone (Fig. 4E, F). Additionally, cortical dysplasia without oligodendroglia-like cells (Fig. 4G) was observed in the lateral temporal region corresponding to the irritative zone (apart from the MRI-lesion in P5).

In P3, the MRI-lesion showed unusual features; namely, multiple small nodules composed of oligodendroglia-like cells within both the cortex and subcortical white matter were evident. The features of nodules did not seem to match the characteristics of specific glioneuronal element, because they lacked mucinous background and floating neurons (Fig. 4H).

However, astrocytic cells with hyperchromatic nuclei and fine processes were observed diffusely with a slight increase in cellularity in the cortex (Fig. 4I), superficial cortical layer (Fig. 4J), and subcortical white matter. No features suggestive of malignancy were evident. Based on the features, we regarded this case (P3) as a DNT-nonspecific form,<sup>7)</sup> where the ictal onset zone and irritative zone were identified within and beyond the MRI-lesion. No histopathologic differences in the areas corresponding to the ictal onset zone, irritative zone, and MRI-lesion (Table 2) were observed. The hippocampus taken from two patients (P4 and P5) showed no sclerosis.

#### IV. Surgical procedures and seizure outcome

Follow-up periods ranged from 34 to 104 months (mean: 75 months) (Table 2). Three patients experienced no seizures after surgery (Engel Class I); two of three (P3 and P4) patients underwent total lesionectomy, and one (P5) underwent partial lesionectomy; complete removal of ictal onset zones and irritative zones were performed in all cases. However, in the remaining two patients (P1 and P2), where the MRI-lesion was totally resected (total lesionectomy) without complete removal of the ictal onset zone and irritative zone due to the functionally eloquent cortex, they experienced residual seizures (Engel Class II and III) after surgery.

### Discussion

#### I. Intracranial-video EEG and histopathologic correlations implying epileptogenicity of DNT

In this study, we evaluated precise correlations

between the cortical topography of histopathologic findings and the epileptic zones of ictal onset zone and irritative zone using extraoperative intracranial-video EEG in patients with DNT.

Electrographically, MRI-lesion was nonresponsive or less active than the surrounding cortex, which was responsible for the epileptic zones of ictal onset zone and irritative zone in four patients (P1, P2, P4, and P5) with simple or complex forms. There was cortical topography of histopathologic features which correlated to the MRI-lesion, and epileptic zones of ictal onset zone and irritative zone. The main component of MRI-lesions was the specific glioneuronal element with or without glial component and calcifications. The specific glioneuronal element formation became less apparent in the surrounding cortex with an ictal onset zone, and alternatively dysplastic cortex appeared with less intermixed oligodendroglia-like cells. Further transition was observed from the dysplastic cortex to the well-preserved cortex in the irritative zone. These results may suggest intrinsic but different epileptogenicity in the cortical topography of DNT pathology, which encompasses not only the MRI-lesion but also the MRI-nonvisible epileptic zones.

As for less excitable specific glioneuronal element, the main component of MRI-lesion with lazy electrical activity on intracranial-video EEG may be related to immature neuronal differentiation of oligodendroglia-like cells, which are derived from progenitor cells capable of both neuronal and glial differentiation.<sup>11,12)</sup> Previous ultrastructural observations have demonstrated that most oligodendroglia-like cells possess a small number of slender processes with deficient synapse formation, while mature neurons with synapse formation are small in number.<sup>11,15)</sup> However, dysplastic neurons are highly epileptogenic in association with ECoG hyperexcitability.<sup>3)</sup> Boonyapisit et al. have elucidated direct ECoG-histopathologic correlations to assess the epileptogenicity expression of focal cortical dysplasia.<sup>3)</sup> Accordingly, they showed a different expression of epileptogenicity in various pathological types of cortical dysplasia. Ictal onset was not found in Type-IIB regions (characterized with balloon cells), despite the presence of severe cortical architectural disorganization and numerous dysmorphic neurons. The most interictal and ictal changes were seen in Type-IIA regions, where the presence of dysmorphic cells and architectural disorganization were apparent. Ictal onset zones were also observed in the Type-I region with the presence of architectural disorganization of the cortical layers but without dysmorphic neurons or balloon cells.<sup>3)</sup> Balloon cells containing cortical dysplasias are characterized with

a signal increase on the FLAIR image, whereas other subtypes of cortical dysplasia are less likely to be MR positive.<sup>2)</sup> Thus, no preoperative MRI correlates are found in terms of epileptogenicity in patients with cortical dysplasia. These results are analogous to our findings, suggesting that intraoperative or extraoperative electrocorticography is required for epileptogenic localization beyond the MRI-lesion in patients with DNT.

P5 had typical cortical dysplasia in an irritative zone remotely sited from the MRI-lesion. In this study, we differentiated the dysplastic cortex in the ictal onset zone and irritative zone from typical cortical dysplasia. The dysplastic cortical areas in the ictal onset zone and irritative zone were intermixed with oligodendroglia-like cells, which are the main constituent cells of specific glioneuronal element<sup>11,12,15)</sup> albeit typical cortical dysplasia lacks other histopathologic components of DNT (e.g., oligodendroglia-like cells).<sup>14,19–21)</sup> Previously, foci of cortical dysplasia have been found in specimens surgically taken from DNT patients.<sup>14,17,24,27)</sup> Previous studies may not have strictly differentiated dysplastic neurons with intermixed oligodendroglia-like cells from typical cortical dysplasia. We attributed the adequate differentiation to locating the intrinsic epileptogenicity of DNT, including the MRI-lesion and surrounding cortex with MRI-negative and DNT-related histopathologic changes (i.e., excluding cortical dysplasia). The ictal onset zone was not found coexisting with typical cortical dysplasia in P5, although localizing this lesion would not be achieved without intracranial-video EEG examination.

In P3 with the nonspecific form DNT, the ictal onset zone and irritative zone were identified within the MRI-lesion, where the dysplastic cortex with oligodendroglia-like cells was evident. The histopathologic features were similar to those of ictal onset zone and irritative zone in the other four patients with simple/complex forms DNT (P1, P2, P4, and P5). As depicted by Daumas-Duport, DNT is a glioneuronal tumor with a wide spectrum of features.<sup>5–7)</sup> In this tumorous lesion, intracranial-video EEG examination was essential for determining the precise epileptogenic location.

## II. Surgical treatment of DNT

In this study, total lesionectomy of the MRI-lesion with additional and possibly complete cortical resection (including ictal onset zone and irritative zone) yielded postoperative seizure freedom (Engel Class I) in three patients. The remaining two patients with lesionectomy per se experienced residual seizure after surgery (Class II and III in one each).

Consensus about the surgical strategy for DNT-related intractable epilepsy has not been established. Several studies support a simple lesionectomy for seizure control based on their seizure freedom rate, although it fluctuates widely between 50% and 90%.<sup>1,6,10,16)</sup> Nolan et al. have evaluated the prognostic features for seizure recurrence in 26 children with DNT.<sup>18)</sup> A 12-month follow-up indicates that 22 children (85%) establish relief of Class I, while residual tumor on postoperative MRI poses as a significant risk factor for poor seizure outcome.<sup>18)</sup> In recent years, others have tended to prefer an extended surgery with ECoG-guided cortical resection for better outcome.<sup>4,17,24,26,27)</sup> They have accomplished ca. 100% (between 90.5% and 100%) of seizure-free rate after extended surgery with the aid of ECoG and/or intracranial-video EEG.

Considering the efficacy of simple lesionectomy, it is important to appropriately and analogously define “lesionectomy.” We defined “lesionectomy” as a resection of the MRI-lesion in the present study. Some authors may define it as gyrectomy; that is, including the tumor and surrounding cortex in the same gyrus.<sup>17,27)</sup> Note that gyrectomy resecting the peritumoral epileptogenic cortex (ictal onset zone and/or irritative zone) can lead to a favorable outcome.

However, the irritative zone is distributed extensively beyond the boundary of sulci, and the histopathologic abnormality may also extend continuously from the main component of MRI-lesion, as noted in this study. Moreover, the foci of typical cortical dysplasia were detected even in the cortex remote from the MRI-lesion. Cortical dysplasia has been frequently detected from the temporal lobe isolated by standard temporal lobectomy in patients with DNT.<sup>27)</sup> Our study supports extended surgery that includes the MRI-nonvisible epileptogenic cortex with intracranial-video EEG monitoring.

## Conclusions

Intracranial-video EEG demonstrated that the ictal onset zone and irritative zone were responsible for epileptogenicity in patients with DNT. Both ictal onset zone and irritative zone were located in the cortex adjacent to the margin of the MRI-lesions. Histopathologic findings of the ictal onset zone and irritative zone revealed that the zones were characterized with dysplastic cortex accompanying a variable number of oligodendroglia-like cells with or without astrocyte proliferation. Both zones were not found in the MRI-lesions. The cortical topography of DNT-related histopathology suggested intrinsic epileptogenicity of DNT. Intracranial-video EEG analysis is warranted to demarcate the appropriate

resection areas for excellent surgical outcome. In view of the small number of patients, further investigation is obviously needed to clarify these findings.

### Acknowledgments

This study was partly supported by Grants-in-Aid for Scientific Research (C) from the Japanese Ministry of Education, Science and Culture (23500481). We are indebted to Dr. Hiroshi Otsubo for valuable discussion and critical review of this article.

### Conflicts of Interest Disclosure

All authors who are members of The Japanese Neurosurgical Society (JNS) have registered online Self-reported COI Disclosure Statement Forms through the website for JNS members. Akiyoshi KAKITA and Koji ARIHIRO are not the member of JNS, who have no potential COI concerning this article.

### References

- 1) Aronica E, Leenstra S, van Veelen CW, van Rijen PC, Hulsebos TJ, Tersmette AC, Yankaya B, Troost D: Glioneuronal tumors and medically intractable epilepsy: a clinical study with long-term follow-up of seizure outcome after surgery. *Epilepsy Res* 43: 179–191, 2001
- 2) Blümcke I, Thom M, Aronica E, Armstrong DD, Vinters HV, Palmini A, Jacques TS, Avanzini G, Barkovich AJ, Battaglia G, Becker A, Cepeda C, Cendes F, Colombo N, Crino P, Cross JH, Delalande O, Dubeau F, Duncan J, Guerrini R, Kahane P, Mathern G, Najm I, Ozkara C, Raybaud C, Represa A, Roper SN, Salamon N, Schulze-Bonhage A, Tassi L, Vezzani A, Spreafico R: The clinicopathologic spectrum of focal cortical dysplasias: a consensus classification proposed by an ad hoc Task Force of the ILAE Diagnostic Methods Commission. *Epilepsia* 52: 158–174, 2011
- 3) Boonyapisit K, Najm I, Klem G, Ying Z, Burrier C, LaPresto E, Nair D, Bingaman W, Prayson R, Lüders H: Epileptogenicity of focal malformations due to abnormal cortical development: direct electrocorticographic-histopathologic correlations. *Epilepsia* 44: 69–76, 2003
- 4) Chan CH, Bittar RG, Davis GA, Kalnins RM, Fabinyi GC: Long-term seizure outcome following surgery for dysembryoplastic neuroepithelial tumor. *J Neurosurg* 104: 62–69, 2006
- 5) Daumas-Duport C: Dysembryoplastic neuroepithelial tumours. *Brain Pathol* 3: 283–295, 1993
- 6) Daumas-Duport C, Scheithauer BW, Chodkiewicz JP, Laws ER, Vedrenne C: Dysembryoplastic neuroepithelial tumor: a surgically curable tumor of young patients with intractable partial seizures. Report of thirty-nine cases. *Neurosurgery* 23: 545–556, 1988
- 7) Daumas-Duport C, Varlet P, Bacha S, Beuvon F, Cervera-Pierot P, Chodkiewicz JP: Dysembryoplastic neuroepithelial tumors: nonspecific histological forms—a study of 40 cases. *J Neurooncol* 41: 267–280, 1999
- 8) Engel J Jr, Van Ness PC, Rasmussen TB, Ojemann LM: Outcome with respect to epileptic seizures, in Engel J Jr (ed): *Surgical Treatment of the Epilepsies*. New York, Raven Press, 1993, pp 367–373
- 9) Ferrier CH, Aronica E, Leijten FS, Spliet WG, van Huffelen AC, van Rijen PC, Binnie CD: Electrocorticographic discharge patterns in glioneuronal tumors and focal cortical dysplasia. *Epilepsia* 47: 1477–1486, 2006
- 10) Giulioni M, Galassi E, Zucchelli M, Volpi L: Seizure outcome of lesionectomy in glioneuronal tumors associated with epilepsy in children. *J Neurosurg* 102 (3 Suppl): 288–293, 2005
- 11) Hirose T, Scheithauer BW, Lopes MB, VandenBerg SR: Dysembryoplastic neuroepithelial tumor (DNT): an immunohistochemical and ultrastructural study. *J Neuropathol Exp Neurol* 53: 184–195, 1994
- 12) Honavar M, Janota I, Polkey CE: Histological heterogeneity of dysembryoplastic neuroepithelial tumour: identification and differential diagnosis in a series of 74 cases. *Histopathology* 34: 342–356, 1999
- 13) Iida K, Otsubo H, Matsumoto Y, Ochi A, Oishi M, Holowka S, Pang E, Elliott I, Weiss SK, Chuang SH, Snead OC 3rd, Rutka JT: Characterizing magnetic spike sources by using magnetoencephalography-guided neuronavigation in epilepsy surgery in pediatric patients. *J Neurosurg* 102 (2 Suppl): 187–196, 2005
- 14) Kameyama S, Fukuda M, Tomikawa M, Morota N, Oishi M, Wachi M, Kanazawa O, Sasagawa M, Kakita A, Takahashi H: Surgical strategy and outcomes for epileptic patients with focal cortical dysplasia or dysembryoplastic neuroepithelial tumor. *Epilepsia* 42 (Suppl 6): 37–41, 2001
- 15) Kordek R, Biernat W, Zakrzewski K, Polis L, Liberski PP: Dysembryoplastic neuroepithelial tumor (DNT): an ultrastructural study of six cases. *Folia Neuropathol* 37: 167–170, 1999
- 16) Lee DY, Chung CK, Hwang YS, Choe G, Chi JG, Kim HJ, Cho BK: Dysembryoplastic neuroepithelial tumor: radiological findings (including PET, SPECT, and MRS) and surgical strategy. *J Neurooncol* 47: 167–174, 2000
- 17) Lee J, Lee BL, Joo EY, Seo DW, Hong SB, Hong SC, Suh YL, Lee M: Dysembryoplastic neuroepithelial tumors in pediatric patients. *Brain Dev* 31: 671–681, 2009
- 18) Nolan MA, Sakuta R, Chuang N, Otsubo H, Rutka JT, Snead OC, Hawkins CE, Weiss SK: Dysembryoplastic neuroepithelial tumors in childhood: long-term outcome and prognostic features. *Neurology* 62: 2270–2276, 2004
- 19) Otsubo H, Hwang PA, Jay V, Becker LE, Hoffman HJ, Gilday D, Blaser S: Focal cortical dysplasia in

- children with localization-related epilepsy: EEG, MRI, and SPECT findings. *Pediatric Neurol* 9: 101–107, 1993
- 20) Palmieri A, Andermann F, Olivier A, Tampieri D, Robitaille Y: Focal neuronal migration disorders and intractable partial epilepsy: results of surgical treatment. *Ann Neurol* 30: 750–757, 1991
- 21) Palmieri A, Gambardella A, Andermann F, Dubeau F, da Costa JC, Olivier A, Tampieri D, Gloor P, Quesney F, Andermann E: Intrinsic epileptogenicity of human dysplastic cortex as suggested by corticography and surgical results. *Ann Neurol* 37: 476–487, 1995
- 22) Rutka JT, Otsubo H, Kitano S, Sakamoto H, Shirasawa A, Ochi A, Snead OC: Utility of digital camera-derived intraoperative images in the planning of epilepsy surgery for children. *Neurosurgery* 45: 1186–1191, 1999
- 23) Seo DW, Hong SB: Epileptogenic foci on subdural recording in intractable epilepsy patients with temporal dysembryoplastic neuroepithelial tumor. *J Korean Med Sci* 18: 559–565, 2003
- 24) Sharma MC, Jain D, Gupta A, Sarkar C, Suri V, Garg A, Gaikwad SB, Chandra PS: Dysembryoplastic neuroepithelial tumor: a clinicopathological study of 32 cases. *Neurosurg Rev* 32: 161–169; discussion 169–170, 2009
- 25) Shirozu H, Iida K, Hashizume A, Hanaya R, Kiura Y, Kurisu K, Arita K, Otsubo H: Gradient magnetic-field topography reflecting cortical activities of neocortical epilepsy spikes. *Epilepsy Res* 90: 121–131, 2010
- 26) Sugano H, Shimizu H, Sunaga S: Efficacy of intraoperative electrocorticography for assessing seizure outcomes in intractable epilepsy patients with temporal-lobe-mass lesions. *Seizure* 16: 120–127, 2007
- 27) Takahashi A, Hong SC, Seo DW, Hong SB, Lee M, Suh YL: Frequent association of cortical dysplasia in dysembryoplastic neuroepithelial tumor treated by epilepsy surgery. *Surg Neurol* 64: 419–427, 2005

---

*Address reprint requests to:* Koji Iida, MD, PhD, Department of Neurosurgery, Graduate School of Biomedical and Health Sciences, Hiroshima University, 1-2-3 Kasumi, Minami-Ku, Hiroshima, Hiroshima 734-8551, Japan.  
*e-mail:* iidak@hiroshima-u.ac.jp